1. The effect of electric field on the deposition of radon daughters and air contaminants on the plant canopy

1.1. Known facts and assumptions

Natural atmospheric radioactivity is determined by the concentration of radon and radon daughter elements in air. Radon daughter elements are carried by aerosol particles of accumulation mode as well as by nanometer particles and clusters (Porstendörfer et al., 2000; Wasiolek and James, 2000). Immediately after the decay of a ^{222}Rn atom the daughter atom ^{218}Po forms a positively charged cluster of nanometer size. The molecular clusters containing ^{214}Pb and ^{214}Bi also have considerable probability to carry positive charge. The charged nanometer clusters are called small air ions in atmospheric electricity. The velocity of electric drift of a small air ion in the fair weather atmospheric electric field is about 1 cm s^{-1} that exceeds the typical deposition velocity of electrically neutral air pollutants.

The effect of electric field on radon daughters is known in atmospheric electric research long time ago. Artificial electric fields have been used for sampling of the radon daughters for measurement since research by Elster and Geitel (1902). The radon daughters are traditionally collected for analysis on a horizontally spanned wire connected to the negative terminal of a HV source. Wilkening (1977) first showed by measurement that the concentration of radon daughter atoms in air is strongly influenced by thunderstorm electric field. Wilkening did not directly measure the deposit of radon daughters on the ground. He showed that the concentration of radon daughters in air has decreased many times in an inverted electric field during a thunderstorm, although the radon concentration remained constant. Willett (1985) thoroughly studied the deposition of radon daughters in relation with the ground-level atmospheric electric electrode effect. His model predicts significant enhancements of the ground surface radioactivity as a result of electric deposition of cluster-carried radon daughters under typical continental conditions. The radioactive deposition itself was not the subject for Willett, who studied the vertical profile of air conductivity near the ground. As a rule, scientists working in field of atmospheric electricity did not consider possible applications of the achieved knowledge in radiation hygiene. As an exception, the effects of the electric field on the deposition of radon daughters and its applications in radiation hygiene have been discussed by Jonassen (1988).

Heated discussion was started by Henshaw et al. (1996), who published an impressive demonstration of the enhanced deposition of radon daughters on the walls in the vicinity of electric power cables indoors, and explained the effect by electric deposition of dust particles carrying the attached fraction of radon daughters. Additionally, Henshaw et al. (1996) pointed to the problem of electrostatic deposition of radon daughters as a possible mechanism of the environmental effect of high voltage (HV) power lines. Miles and Algar (1997) published a first objection to Henshaw et al. They measured the concentration of radon daughters under a 400 kV power line and showed no considerable increase of concentration at a height of 0.6 m over grass directly under the line conductors. This objection by Miles and Algar seems irrelevant because Henshaw did not claim an increase of concentration of radon daughters in air. To the contrary, deposition should rather decrease their concentration in air, but this effect is estimated too weak to be detected by measurement at the height of 0.6 m under alternating current (AC) lines. Afterwards Fews, Henshaw et al. (1999b) showed that the AC power line is able to produce a moderate direct current (DC) electric field on the ground and that electric deposition of radon daughters could be detected under HV power lines (Fews et al. 1999a).

Jeffers (1999) explained the effect of electric field on the surface radioactivity with deposition of unattached fraction of radon daughters. The measured effects of electric

deposition of cluster ions agree with theoretical calculations by Willett (1985). Henshaw expected opposite that the radon daughters are carried by neutral or low mobile aerosol particles. Electric deposition of aerosol particles could be an effect of wide environmental importance because the particles carry not only radon daughters but also an essential part of miscellaneous air pollutants. The electric mechanism of deposition has been often neglected because the electric mobilities of aerosol particles are three orders of magnitude less than the mobilities of small ions, and the particles are not unipolar charged. In the natural atmospheric environment, the electric field is weak and airborne particles are neutral or weakly charged due to thermal fluctuations of electrostatic energy. Thus the electric forces acting on airborne particles in the atmosphere are weak and often neglected when discussing the dry deposition of these particles. In the recent review of dry deposition by Weseley and Hicks (2000) electric mechanism is not mentioned at all. The role of electric force in particle deposition is largest when dealing with the carriers of radon daughter elements. Porstendörfer (1994) has compiled a respected review of the behavior of radon progeny in air. Considering the mechanisms of dry deposition, Porstendörfer writes: “In general, the dry deposition of aerosol particles is governed by the physical processes of sedimentation by gravity, impaction by inertial forces, interception and Brownian diffusion”. The electric mechanism is neglected despite its being most obvious in case of deposition of radon daughters. Electrostatic deposition of particles is well known in technical applications, e.g. electrostatic filters and samplers. It is known a device where electric field is used for cleaning of the air from radon daughters (Moeller, 1986). Strong electric field and artificial charging of particles occur in these devices. Schneider et al. (1994) showed how aerosol particles are deposited on the faces and eyes of people exposed to a strong electric field, e.g. near a computer display.

The effect of electric field on the deposition of particles on a plane surface appears weak. However, some other weak factors, e.g. gravitational sedimentation, are never neglected when discussing the dry deposition of particulate matter from air. Electric force applied on a single charged particle is Ee, where E is electric field and e is elementary charge. The electric force is superior to gravity when the particle diameter is less than the critical size

$$d_{gE} = \sqrt[3]{\frac{6Ee}{\pi\rho g}}, \qquad (\#.1)$$

where ρ is the particle density and g is the acceleration due to gravity. The critical size of water droplets in the normal fair weather electric field (E = 150 V m^{-1}) is 167 nm. The number of airborne particles of diameter less than 167 nm exceeds the number of bigger particles. Thus the electric force surpasses the gravitational force for most airborne particles. When comparing the electrostatic and diffusion deposition the fact should be considered that diffusion coefficient of aerosol particles decreases simultaneously with electric mobility and the relative effect of electric field could appear considerable (Tripathi and Harrison, 1998).

The long-living radon daughters ^{210}Pb, ^{210}Bi, and ^{210}Po enter into composition of aerosol particles, and also ^{214}Pb and ^{214}Bi may be found in the aerosol phase. As estimated, about 50% of the alpha-radioactivity of air is carried by air ions of high mobility, the other 50% is carried by aerosol particles that are electrically neutral or of low mobility. Therefore, both the ionic deposition and the deposition of aerosol particles are important in the nature. The known theoretical calculations are insufficient to decide under which conditions the electric deposition of aerosol particles could be neglected or should be considered. In the present research a simple theoretical model is developed and used to identify the conditions which require that the electric field should be accounted when analyzing dry deposition of particulate matter from atmospheric air.

It has been determined that molecules of some non-radioactive substances in atmosphere also have considerable probability to be in the composition of air ions. The charging probability of molecules with high electron or proton affinity may be up to 10^{12} times larger

than that of non-active molecules. Considerable amount of polluting substances in air are presented in the aerosol phase and electric field can control their deposition on the sharp edges of electrically grounded bodies. Unlike the diffusion deposition, the electrostatic deposition is essentially non-uniform: the plate out on the tips of leaves and conifer needles is much more intensive than on hidden surfaces of the plants. That is why the effect of electric field on the deposition of non-radioactive substances on vegetation is worth of attention. The known fact that the top branches of conifers are first of all damaged by chemical pollution has no definite explanation up to now. The knowledge of the deposition geometry of radioactive elements and aerosol particles would help to understand the factors of pollution damages and the propagation of polluting substances, including radioactivity, in biologic cycles.

1.2. Electric field

1.2.1. Natural atmospheric electric field

Strong electric field is generated by thunderstorms. The thunderstorm currents charge the ionosphere-ground capacitor up to 200–300 kV. As a result, electric field is permanently present in the atmosphere. Average strength of the fair weather atmospheric electric field near the ground is typically 100–150 V/m dependent on the measuring site. When estimating the role of the electrostatic deposition in nature, the frequency of different values of the electric field should be known. Statistical distribution of electric field is analyzed using the measurements in Marsta Observatory, Sweden, that have been carried out by Uppsala University in co-operation with Tartu University. At Marsta Observatory, the air electric conductivity, electric field and near-ground space charge density are recorded on the computer carrier continuously from 1993. Since 1994 the data have been complemented with continuous recordings of meteorological parameters. The database gives some new possibilities for analysis of the regularities of variations of fair weather atmospheric electricity.

The Marsta Observatory (59°56’N, 17°35’W) is located in rural area 10 km north of Uppsala. The surroundings are a very flat farming field. Nearest forest is located more than 1 km from the observatory, which provides undisturbed micro-meteorological conditions. There are no industrial establishments around the observatory. The closest sources of possible air pollution are the town of Uppsala and a military airport with infrequent air traffic situated between the observatory and the town. The small two-storied observatory building is heated by electric power. The soil around the observatory is relatively rich in radium and is loosened in the process of cultivation of the land every year. Thus the concentration of radon around the observatory is relatively high, which results in high air conductivity and a low electric field. Statistical characteristics of electric field are presented in Table #.1 and histogram of distribution in Figure #.1.

Table #.1

Atmospheric electric field at Marsta Observatory according to statistics of 46608 hours

Parameter	Electric field
1% percent point	-627 V/m
25% percent point	35 V/m
median	67 V/m
75% percent point	98 V/m
99% percent point	231 V/m
average	51 V/m
standard deviation	142 V/m

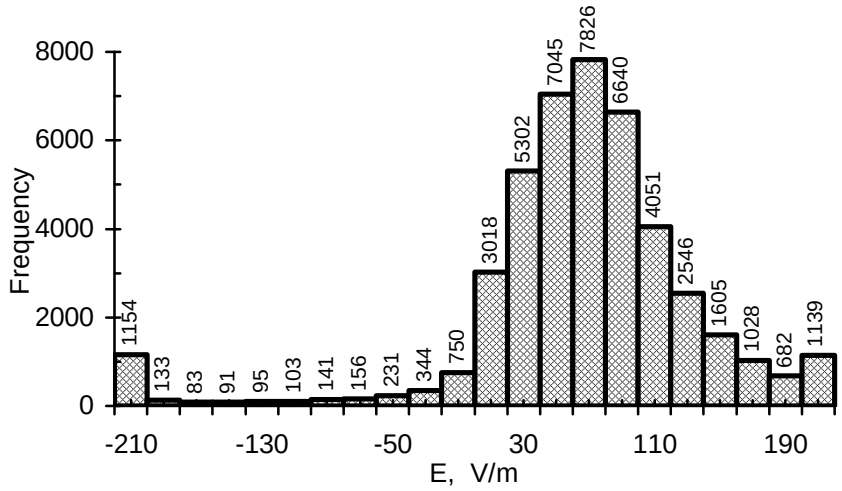

Figure #.1. Atmospheric electric field at Marsta Observatory according to statistics of 46608 hours. The edge bars contain all out-of-scale measurements

In most of atmospheric electric stations the average value of electric field is about 2 times higher but the shape of statistical distribution is similar. According to the atmospheric electric tradition the electric field is considered positive when directed downwards and the ground carries negative charge. The distribution histogram shows that most of the time the electric field is positive and the positive ions that carry the radioactivity are drifting downwards. Extreme values of electric field are characteristic of thunderstorm situation. During the thunderstorms, negative electric fields are prevailing and in this case the effect of electrostatic deposition of positive ions is switched off.

1.2.2. Electric field under a HV power line

The electric field induced by ordinary power transmission line is alternating and does not enforce a directed flux of ions. The ions are oscillating in the AC electric field with low amplitudes and the field does not force the deposition of ions on the plain surfaces. However, the AC electric field is still a factor of deposition when the deposition target is fine needle or grass haulm because the air is carried by wind and residence time of the air in the deposition zone near the needle is typically less than the period of the oscillation.

Corona discharge that is characteristic of HV power lines generates the space charge near the wires and simplified electrostatic calculation of the field ignoring the space charge yields incorrect results. Theoretical consideration of corona effect on the electric field is complicated. Thus the reliable results can be achieved by measurement. The measurement were carried out under the same power line where the deposition of radon daughters was studied. The instrument was designed as a ground level horizontal plate antenna. The parameters of the line: number of parallel conductors 3, distance between the conductors 9.2 m, height over a flat ground 10.2 m, voltage 330 kV, frequency 50 Hz. The field was measured on one side of the line and complemented for the other side by symmetry. Result is shown in Figure #.2.

The amplitude of electric field under HV power line is about the same as the maximum value of the natural atmospheric electric field in thunderstorm situation. The ions of mobility 1.27 $cm^2V^{-1}s^{-1}$ oscillate in a field of 8000 V/m with a velocity of 1 m/s and amplitude of 3.2 mm. It could result in some enhancement of deposition on the salient objects like tree leaves and needles.

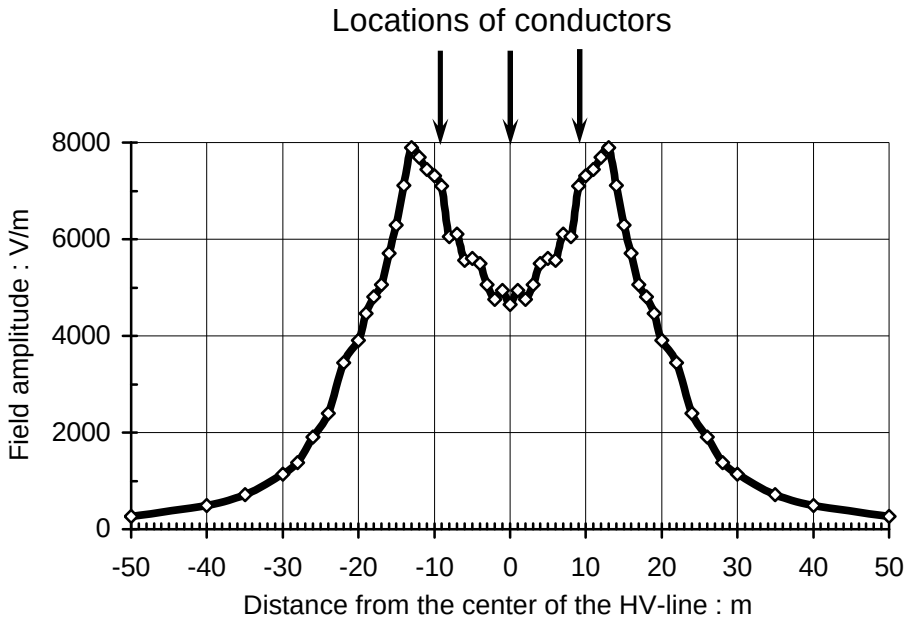

Figure #.2. Electric field under a 330 kV power line according to measurement

1.3. Deposition of radon daughters on spruce needles

1.3.1. The test model for theoretical estimates

The electric field is strongly enhanced on the tips of leaves and on needles of plants. Therefore the electric deposition of cluster ions and particles to elements of plants depends on the geometry of plants. It follows that the electric field could bias the distribution of deposit on the elements of plants and in this manner it could control air pollution damage. The shapes and positions of leaves and needles are variable and an exact calculation of the distribution of deposit seems a hopeless task. A simplified model needs to be considered to allow rough theoretical estimates about the importance or otherwise of the electric mechanism of deposition of particles to plants.

According to intuitive geometric considerations, the strongest electric field is expected on needles of conifer trees, especially on the top of the tree. A needle can be modeled as a piece of thin cylinder. A thin cylinder is a proper model as well for grass or cereal reeds. Thus a thin and long cylinder or wire is chosen below as a model target of deposition. The electric field on a surface of a wire depends of the distribution of the grounded elements around it. The geometry of the surrounding elements in a real plant canopy is variable and too complicated to make exact calculations. A simple geometric object should be used as a model of the surrounds. The effect of electric field is most significant when the needle or reed is positioned over the open surface of plant canopy. A grounded plane placed parallel to the wire models this situation. The distance from the wire to the plane should be chosen as comparable with the distance from the needle or reed to the neighboring elements of plants. The model is illustrated in Figure #.3.

Uniform and perpendicular to the wire airflow is assumed in the neighborhood of the wire. The wind speed near the wire v differs from the meteorological wind speed and should be estimated considering the actual location of the deposition target.

The electric field on the surface of a long wire of radius R distant H from the plane is

$$E = \frac{H}{R\ln(2H/R)} E_o, \qquad (\#.2)$$

where E_o is the undisturbed atmospheric electric field over the plane. The field on the surface of a short needle is slightly stronger than the estimate above. The enhancement of the atmospheric electric field on the wire is described by the ratio E/E_o, which could reach values up to one hundred. An example: if R = 0.5 mm and H = 7 cm then E = 25 E_o.

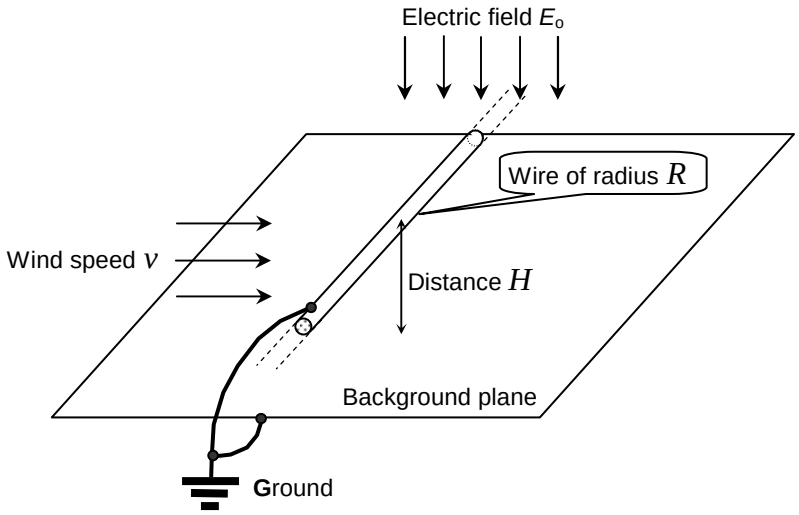

Figure #.3. Diagram of the test model.

The model of the target of deposition as a wire spanned over a plane surface is a very rough approximation to the real geometry of plant structures. Thus the model does not claim to give precise results and there is no need for strong requirements for the exactness of calculation of the electric and mechanical depositions of particles on the model wire.

1.3.2. Factors of deposition of cluster ions

The effect of gravity and inertia of clusters is negligible and their deposition is controlled by two factors: Brownian diffusion and drift in electric field. The electric factor is easy to estimate because the cluster ions are single charged and electric mobility Z is their indirect characteristic. The electric deposition velocity u_E of cluster ions is:

$$u_E = EZ\ . \qquad (\#.3)$$

The Brownian deposition on a cylinder is estimated using the well-proven Churchill-Bernstein equation of heat transfer from a wire (see Incropera and DeWitt, 1996)

$$\mathrm{Nu} = \left(0.3 + \frac{0.62\,\mathrm{Re}^{1/2}\,\mathrm{Pr}^{1/3}}{\left(1+(0.4/\mathrm{Pr})^{2/3}\right)^{1/4}}\right)\left(1+\left(\frac{\mathrm{Re}}{282000}\right)^{5/8}\right)^{4/5}, \qquad (\#.4)$$

in which there are three dimensionless parameters:

the Nusselt number $$\mathrm{Nu} = \frac{2Rh}{\kappa}\ , \qquad (\#.5)$$

the Reynolds number $$\mathrm{Re} = \frac{2Rv}{\nu}\ , \qquad (\#.6)$$

the Prandtl number $$\mathrm{Pr} = \frac{\nu}{a}\ . \qquad (\#.7)$$

The symbols used above are: h – coefficient of heat transfer, κ – thermal conductivity of air, ν – kinematic viscosity of air, and a – thermal diffusivity of air. Equation (12) may be translated according to Eckert and Drake (1972) to terms of the Brownian diffusion. The translation consists of two substitutions:

the Nusselt number by the Sherwood number

$$\mathrm{Sh} = \frac{2Ru_D}{kTB} \ , \qquad (\#.8)$$

and the Prandtl number by the Schmidt number

$$\mathrm{Sc} = \frac{\nu}{kTB} \ , \qquad (\#.9)$$

where k is the Boltzmann coefficient, T is absolute temperature, and B is the mechanical mobility of clusters. The diffusion coefficient is replaced above by the term kTB on the basis of the Einstein law (see e.g. Fuchs, 1964). The mechanical is related to the electric mobility. If the charge of the cluster is supposed e, then

$$Z = eB. \qquad (\#.10)$$

If the condition Re Sc > 0.2 is satisfied (and it is well satisfied, as a rule), the translated equation offers a good approximation:

$$u_D = \frac{kTB}{2R}\left(0.3 + \frac{0.62\,\mathrm{Re}^{1/2}\,\mathrm{Sc}^{1/3}}{\left(1+(0.4/\mathrm{Sc})^{2/3}\right)^{1/4}}\right)\left(1+\left(\frac{\mathrm{Re}}{282000}\right)^{5/8}\right)^{4/5} . \qquad (\#.11)$$

1.3.3. Theoretical comparison of Brownian and electric deposition

The ratio of two components of deposition velocity u_E and u_D depends on the wind. The wind speed should here be measured in the immediate vicinity of the deposition target and it depends on the location of the target. The wind speed near the grass reeds of lower branches of trees is essentially less than that at a height of about 10 m as measured by meteorological stations.

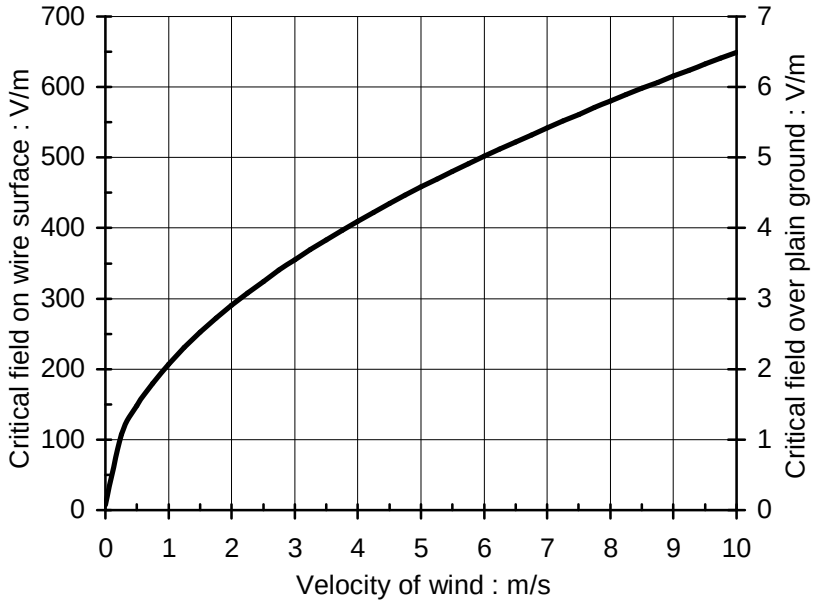

Figure #.4. Critical value of the electrostatic field. When the field exceeds the critical value, the electrostatic deposition exceeds the diffusion deposition. Conditions assumed in the example: $2R$ = 1 mm, D = 0.03 cm^2 s^{-1}, Z = 1.27 cm^2 V^{-1}s^{-1}, H = 36 cm.

Brownian deposition increases with wind but the electric deposition remains unchanged. It is possible to find the wind speed at which the two factors are equal. This specific wind speed is called the critical wind speed. When actual wind speed exceeds the critical value then the Brownian deposition occurs to be leading mechanism. Electric deposition is leading mechanism at lower wind speeds. Figure #.4. is compiled according to equations above. The natural atmospheric electric field over the plain ground is about a hundred volt per meter and when considering the test model, the electric factor always dominates over Brownian diffusion because the wind speed near the needles is never high enough to cause the critical field exceed the normal atmospheric electric field.

1.3.4. Measurements by means of gamma-spectrometer

The radon daughter elements can be analyzed as according to their alpha–radiation as according to beta- or gamma–radiation. The advantage of gamma-spectrometry is high resolution that enables to identify the isotopes. Gamma-activity of the sample was measured using EG&G Ortec HPGe detector GEM-35200, analyzer 92x-W3 Spectrum Master, and Maestro software. The thoron daughter ^{212}Pb was identified according to the 238.6 keV γ-line and radon daughter ^{214}Bi according to the 609.5 keV γ-line. It was possible to identify as well the long-living daughter of radon^{210}Pb, but interpretation of the results would be difficulty as part of ^{210}Pb has different origin. The method of gamma-spectrometry enables to use large samples of spruce needles. This supports the sensitivity and accuracy of measurements. On the other hand, the requirement of large sample does not enable to learn some details e.g. the radioactivity of tips of needles.

Figure #.5. Spruce under the HV power line used in the experiment. Veljo Kimmel is standing before the spruce.

Table #.2. presents a typical example of measurement results. The spruce needles were picked during 11–13 August 1998 from four locations. The sampling place under the HV line is shown in Figure #.5. The 330 kV line above the spruces was the same as in the electric field measurement described above. The height of conductors from the ground was about 10 m. The electric field on the top of the tree was not measured. A rough estimate gives the field

strength close to the corona discharge field. The sampling place in the natural field was far away from HV lines. The weather during the sampling period was windy with developed turbulence. The needles were picked from a selected branch and put into a calibrated vessel. The amount of needles in different samples varied from 30 to 50 g. A sample was prepared and carried to the laboratory as quickly as possible. The measuring began 780-1020 s after the spruce branch was cut.

Table #.2.

Example of results of gamma-spectrometric measurements

Sample	Radon daughter ^{214}Bi, Bq/kg	Thoron daughter ^{212}Pb, Bq/kg
Top of the spruce under HV line, height from ground about 6 m.	1350	300
Inside of the crown of the same spruce, height from ground about 2 m.	120	measurement is missing
Top of a branch jutting far out in the natural electric field, height from ground about 3 m.	480	35
Inside of the crown of the same spruce, height from ground about 2 m.	215	13

1.3.5. Measurements by means of alpha pulse chamber

The half-life of ^{218}Po is short and the instrument for measurement of alpha-activity of conifer needles and tips of leaves must allow fast manipulation with fresh samples. A special air ionization chamber was designed and manufactured for measurements during this research. A sample is to be placed on the bottom of a 340 cm^3 cylindrical vessel switched for measurement to the potential of +1200 V. Ions created by α-particles are collected on the upper disk electrode connected to an amplifier. Typical length of a pulse is 40–80 ms and it depends on the energy of the particle. Figure #.5. shows distribution of pulse lengths in a experiment where radioactivity of tips of tree leaves was measured. However usage of the pulse length as a measure of energy does not provide satisfactory resolution. Thus the instrument was used to measure the integral alpha-activity of a sample and not as a spectrometer. The time to pick the needles or leaves, cut off their tips and place them into the pulse chamber should not exceed few minutes. Thus the samples are small, typically about hundred milligrams. When measuring the radioactivity of small samples of plant fragments picked from naturel environment, the counting rate and coincidence probability is low.

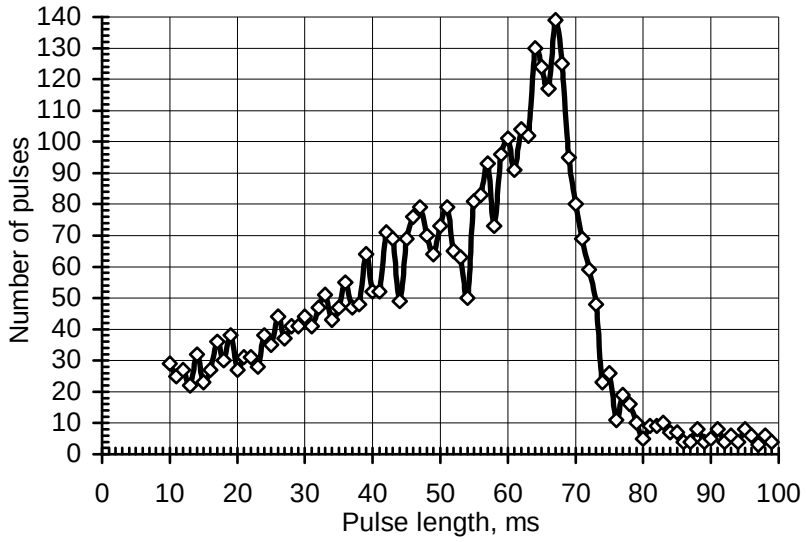

Figure #.5. The distribution of the lengths of pulses in the pulse ionization chamber

The pulse ionization chamber should be used close to the site where the plant fragments are picked. Thus wrong pulses induced by mechanical microvibrations are hard to avoid. According to special measurements with empty chamber the perturbation pulses are shorter than 40 ms. Thus only the pulses longer than 40 ms were counted at actual measurements, which eliminates some short-track alpha pulses as well and slightly reduced the efficiency of the instrument. The alpha particles are counted from an angle about 1 sr. The recording system has about 20% of dead time. Some needles on the bottom of the vessel overlap each other. Considering the losses, the counting efficiency is roughly estimated as about 5% of the radioactive decay events on the needles. Efficiency for background radon in the air is higher and is estimated as about 25%.

An experiment carried out using the alpha pulse chamber is explained below. Two samples were taken from the top of the same spruce under the HV line as in the case of gamma spectrometric measurement, August 10 and 11, 1998. Only the tip fragments of needles were cut and included in the sample. The mass of a sample was less than 0.3 g in order to reduce the overlapping of needles. Sample no. 1 was measured during two hours and sample no. 2 with interruptions during three days. Half-hour counts for sample no. 2 are shown in Figure #.6. The shape of the decay curve is a result of combination of three processes: decay of radon daughters, decay of thoron daughters, and decay of radon in the volume of the vessel. The thoron daughters ^{212}Pb and ^{212}Bi have a combined decay time constant of about 1000 minutes. The constant background radiation is estimated to be about 20 pulses per hour and the sampled thoron daughter pulses about 50 pulses in the first hour. The background can be explained by room radon concentration of about 20 Bq/m^3.

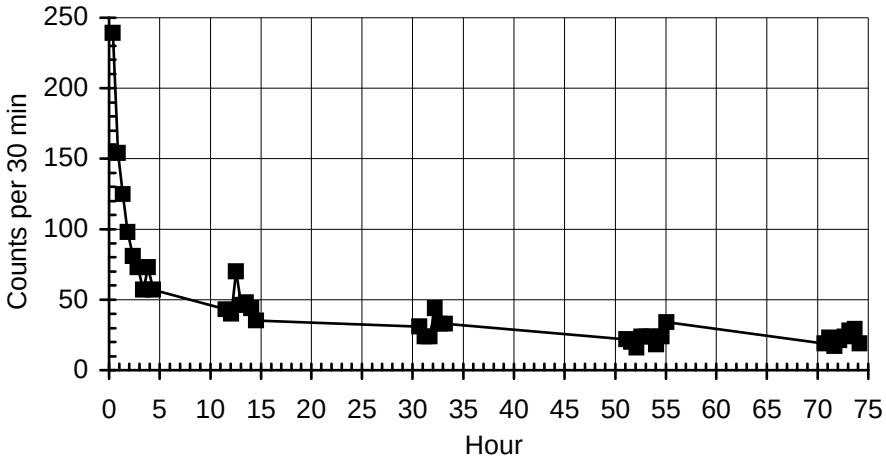

Figure #.6. Decay curve for a sample of spruce needles.

The decay curves are nearly the same for both samples. Thus the radioactivity of needles was estimated by analyzing the sum of counts for the two samples during first hours of measurements. The decay curve for this period is presented in Figure #.7.

The initial activity of radon daughters (without ^{218}Po) in the joint sample is estimated according to analysis of described measurement as about 14 kBq/kg. There was 250 needle fragments in the vessel with total length of 133 cm, and surface area of needle fragments was 28 cm^2. The estimated specific surface activity is about 3 kBq/m^2 that is unusually high value for biologic subjects.

The radon and thoron daughter activities in the alpha-activity measurements are higher than in the gamma spectrometric measurements. The results can be explained in terms of different ways of sampling. In the case of gamma measurements full needles were picked as from the very top of the tree as well as from distances up to 20-30 cm from the top. In the case

of alpha measurements, only the absolute top needles were picked and only the tip fragments were taken into the sample.

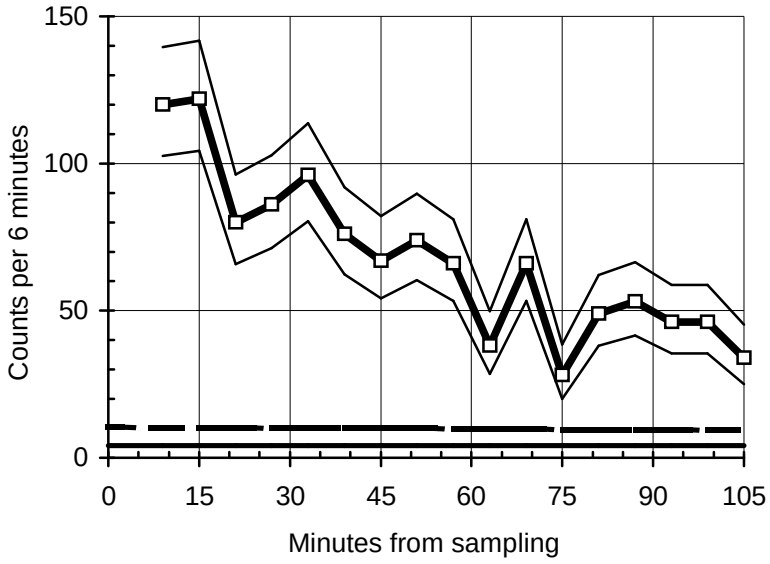

Figure #.7. Counts per 6 minutes for the two samples of needles with the total mass of 0.47 g. Thin lines show the 90% fiducial corridor for Poisson distribution. Lowest line displays the constant background and the dashed line displays the pulses from the thoron daughters. The estimated initial activity of ^{214}Po (RaC´) is about 20 counts per minute. The activity of ^{214}Bi is nearly the same.

Selected results of alpha-measurements are presented in Table #.3. The results confirm the hypothesis about the role of electric field in deposition of radon daughters on trees.

Table #.3.

Alpha-activities of some samples of spruce needles measured by pulse ionization chamber

Sample*: needle fragments from …*	kBq/kg
… the top of a 6 m high spruce below of 330 kV AC line	5 – 20
… an internal branch of the same spruce	< 0.5
… the top of a 6 m high spruce away of 330 kV AC line	5
… the top of a 1.5 m high spruce in natural 120 V/m DC field	3
… the top of a 1 m high spruce connected to –1800 V	20 – 200
… the top of a 1 m high spruce connected to +1800 V	0.4

1.4. Deposition of aerosol particles onto sharp structures

1.4.1. Estimate of electric deposition

The deposition intensity is measured by the deposition velocity defined as the ratio of the deposition flux to the surface area. The electric deposition velocity u_E of uniformly charged particles over a plane surface is easy to estimate:

$$u_E = EZ = EqB, \tag{\#.12}$$

where E is the electric field, q, B, and Z are respectively the electric charge, and mechanical and electric mobilities of the particle. The mechanical mobility is a known function of the particle size (Fuchs, 1964; Tammet, 1995). The above estimate is valid for particles of one polarity. Particles of the other polarity are repelled from the surface by the electric force and do not deposit.

If the particles are not uniformly charged, the probability p_i of a particle to carry the charge $q = ie$ (e is the elementary charge, charge number i is negative for negative particles, zero for neutral particles and positive for positive particles) should be determined first. Thereafter the deposition velocity needs to be calculated as a sum of partial deposition velocities of particles of different charges. The sum is expanded over one polarity since the particles of opposite polarity are repelled from the collecting surface.

The charge probabilities p_i depend on many factors. The equilibrium statistical distribution of particle charges is explained by thermal fluctuations of electrostatic energy (Fuchs, 1964). Hoppel and Frick (1990) gave an improved calculation of charge probabilities. In the present research, exactness requirements are not high and a simple mathematical approximation proposed by Tammet (1991) and refined using data by Reischl et al. (1996) is employed. First the partial coefficients of attachment β of a positive small ion to the particle with charge ie and diameter d are calculated:

$$\left.\begin{aligned} x &= \frac{ie^2}{2\pi dkT\varepsilon_\circ} \\ \beta_i(d) &= 2\pi dkTB\frac{x}{\exp(x)-1}\sqrt{1-\frac{2}{2+i(i-1)+d/(10\text{nm})}}, \quad i=-\infty\ldots+\infty \end{aligned}\right\}. \tag{\#.13}$$

Here k is the Boltzmann constant, T is absolute temperature, and ε_o is the permittivity of vacuum. Next, the unnormalized particle numbers are calculated

$$N_o(d) = 0, \quad N_i(d) = \prod_{j=1}^{i}\frac{\beta_{j-1}(d)}{\beta_{-j}(d)}\Lambda, \tag{\#.14}$$

where Λ is the ratio of air polar conductivities: λ_+/λ_- in case of positive values of i and λ_-/λ_+ in case of the negative values of i. The normalized probabilities are

$$p_i(d) = \frac{N_i(d)}{1+2\sum_{j=1}^{\infty}N_j(d)}. \tag{\#.15}$$

The velocity of electric drift of a particle is $ieBE$ and the field on the surface of the cylinder is given by Equation (2). Therefore the partial deposition velocity of i-charged particles is

$$u_{Ei} = ieB\frac{H}{R\ln(2H/R)}E_o. \tag{\#.16}$$

Finally the electric component of deposition velocity is calculated as a weighted sum of partial deposition velocities

$$u_E = \sum_{i=1}^{\infty}p_i(d)u_{Ei}, \tag{\#.17}$$

which accounts for particles of one polarity. The polarity should be chosen depending on the direction of the electric field. Positive particles move downwards in a normal fair weather atmospheric electric field. Therefore, Equation (8) is written above for positive particles.

1.4.2. Estimate of mechanical deposition

The role of electric field in deposition of particles is characterized by the ratio of the velocities of electric to nonelectric deposition. The nonelectric factors of deposition as listed by Porstendörfer (1994) are sedimentation by gravity, impaction by inertial forces, interception and Brownian diffusion. All these four mechanisms are mechanical in essence and their summary effect will be called mechanical deposition. Specific deposition velocities caused by gravity, aerodynamic effect (impaction and interception) and Brownian diffusion are denoted below by u_G, u_A, and u_D.

The velocity of Brownian deposition is estimated above when considering the deposition of cluster ions.

The gravitational deposition velocity u_G of particles is:

$$u_G = mgB\,, \tag{\#.18}$$

where g is the gravitational acceleration, m and B are respectively the mass and mechanical mobility of the particle.

The aerodynamic deposition of particles of radius r on a cylinder of radius R is estimated in terms of a simplified model. The empirical data presented by Fuchs (1964) and numerical results by Wessel and Righi (1988) are roughly fitted with the equation

$$u_A = \left[\left(\frac{\mathrm{Stk}}{0.6+\mathrm{Stk}}\right)^2 + \frac{r}{R}\right]\frac{v}{\pi}, \tag{\#.19}$$

where v is the air flow velocity and Stk is the Stokes number:

$$\mathrm{Stk} = \frac{vmB}{R}\,. \tag{\#.20}$$

The three specific deposition velocities characterizing different deposition mechanisms are not exactly additive. A rough approximation is used in calculations below to estimate the combined mechanical deposition velocity u_M:

$$u_M = \sqrt{u_G^2 + u_A^2 + u_D^2}\,. \tag{\#.21}$$

1.4.3. Discussion

The role of a specific mechanism of deposition depends not so much on the absolute value of the specific component of deposition velocity as on the relation between the different components of the deposition velocity. The velocity of electric deposition is proportional to the electric field while the other deposition velocities do not depend on the electric field. In a thought experiment the electric field can be adjusted so that the velocity of electric deposition equals the velocity of some other specific deposition. This particular strength of electric field will be called the critical field strength of electric deposition. Different critical electric field strengths can be associated with the gravitational, Brownian, aerodynamic, and joint mechanical depositions.

The concept of critical field strength is helpful when it is necessary to decide on the significance of the electric mechanism of deposition. Electric deposition of aerosol particles can be neglected if the estimated critical field is much higher than the actual atmospheric

electric field, but should be considered an important factor of dry deposition in the opposite case.

The actual atmospheric electric field depends on meteorological conditions. Typical fair weather atmospheric electric field near the ground is 100–200 V m^{-1} while the maximum values exceed 10 kV m^{-1} in thunderstorm situations (see e.g. Israël, 1973). In some situations the anthropogenic electric fields are important, e.g. an AC field of many kV m^{-1} occurs near high voltage power lines.

The value of the critical field can be estimated as a root of the equation $u_E = u_x$, where u_x is a specific velocity of the considered nonelectric mechanism of deposition. The components of deposition velocity can be estimated using the equations derived and presented above. The value of the critical electric field depends on many factors. Most essential factors are the particle size, the wind velocity, the wire diameter, and the distance to the zero-potential surface.

Some decisions about the role of electric deposition can be made by examining typical example situations. An example is considered below. The fixed data that correspond to a typical situation are:

- air parameters match the standard conditions,
- airborne particles are monodisperse spheres,
- wire diameter is 1 mm and distance from zero-potential surface is 7 cm,
- particle density is 2 g/cm^3,
- ratio of air polar conductivities is $\lambda_+/\lambda_- = 2$.

In free atmosphere the air polar conductivities are approximately equal. The ratio of 2 is chosen to match the electrode effect near the ground (see e.g. Israël, 1973).

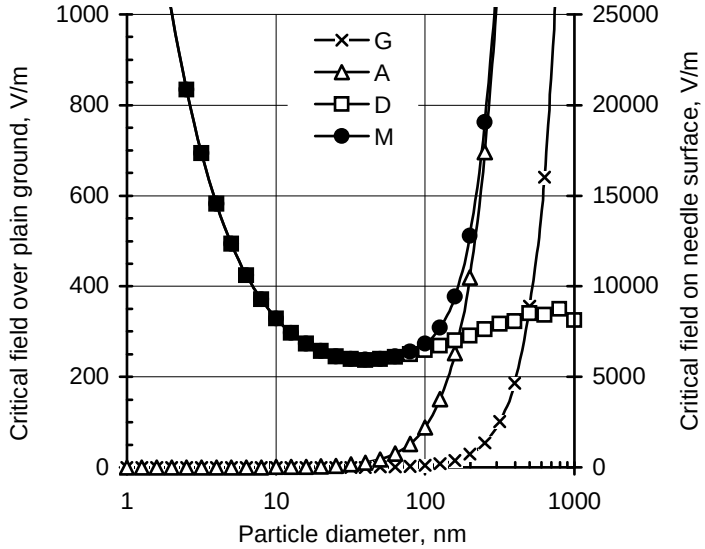

Figure #.8. Critical electric field associated with different mechanisms of deposition: G – gravitational, A – aerodynamic, D – diffusional, M – joint mechanical. Wind speed is 1 m s^{-1}, other assumptions are explained in the text.

The comparison of electric deposition with different specific mechanisms of deposition in low wind situation is given in Figure 2. The critical field associated with gravitational deposition is low for fine particles and reaches the value of an average atmospheric electric field at particle diameters over 100 nm. Thus the electric deposition dominates over the gravitational deposition for most of the atmospheric aerosol particles. If the gravitational

mechanism of deposition of fine particles from atmosphere is the subject of discussion, then the electric mechanism should not to be neglected. This conclusion holds not only for the deposition on needles, but on a plane surface as well.

Aerodynamic deposition is an essential mechanism of deposition of particles of diameter above 100 nm. Aerodynamic sedimentation exceeds electric deposition over a wider size range than gravitational deposition. However, the electric effect dominates over the aerodynamic effect in case of ultrafine particles.

Brownian diffusion is an essential mechanism of deposition of ultrafine particles. It replaces the aerodynamic deposition as the main mechanical deposition mechanism for nanometer particles. The transition size range of 10–200 nm appears to be just the range where the electric effect is most important for dry deposition. In case of uniformly charged particles, the electric mobility and diffusion coefficient are proportional to each other. Thus the dependence of the critical electric field on the particle size is weak in the size range over 10 nm. In case of smaller particles the percentage of the charged fraction of aerosol particles decreases and so does the role of electric deposition when compared with the Brownian deposition.

The example given in Figure 2 shows that while the electric mechanism of dry deposition of particulate matter does not dominate under normal atmospheric conditions, it is comparable with Brownian and aerodynamic mechanisms in the particle size range of 10–200 nm and should not be neglected under the low wind condition.

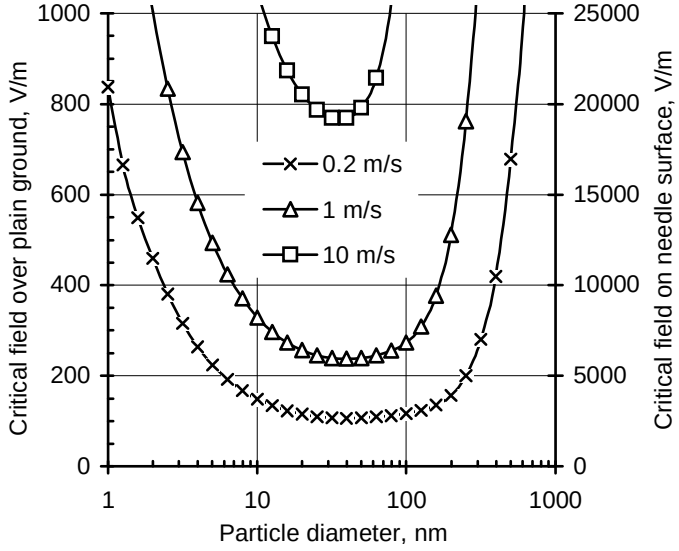

Figure #.9. Critical electric field associated with joint mechanical deposition depending on wind velocity. Assumptions are explained in the text.

The role of electric deposition depends essentially on wind velocity. Wind increases the role of aerodynamic deposition and suppresses the relative role of the electric mechanism. Figure 3 compares the electric deposition to the joint mechanical deposition for different wind velocities. The critical field strength is still lowest for the particle diameter range of 10–200 nm independent of wind. This size range contains most of the atmospheric aerosol particles. In case of low wind of about 1 m/s or less, the critical field is comparable to the normal atmospheric electric field, and electric deposition of aerosol particles has considerable role as a factor of redistribution of deposit on different elements of plants. In a strong wind of about 10 m/s or more, electric deposition can be important only in a thunderstorm situation or on the top branches of trees.

A subject of public discussion is the possible environmental effect of HV power lines. As a rule, power lines transmit AC current. The amplitude of the AC electric field is measured up to ten kilovolts per meter in the vicinity of an HV power line. The possible effect of an AC field on electric deposition is usually neglected as it causes only oscillation and does not enforce any directed flux of charged particles. Fews et al. (1999b) have shown that an AC power line can create a DC field of a few hundred V m^{-1} induced by corona ions. This field is comparable with the natural atmospheric electric field at distances downwind up to half a kilometer from the line. To neglect the AC field as a factor of particle deposition is, however, not correct. The amplitude of oscillation of particles in the AC field of a power line is a fraction of a millimeter. The effect of the oscillating field makes it appearance when fine geometric targets are considered. The time of passage of particles carried by wind through the capture zone near the tips of needles or leaves is essentially less than the period of the field oscillation. Thus the effect of electrostatic deposition of particles on the leaf or needle tips should be nearly the same as in a DC field. The expected environmental effect of HV power lines is the redistribution of the deposit of air pollutants between the tips and shielded surfaces of leaves and needles of plants.

1.5. Conclusions

The effect of atmospheric electric field on deposition of radon daughters carried by positive cluster ions is well known in atmospheric electricity but ill known in radiation hygiene and environmental protection. The research in atmospheric electricity has been concentrated on the effect of radon daughters on air conductivity and the distribution of the deposit on the plant canopy was not studied. The measurements performed in the present research show that electric field is essential mechanism controlling the deposition of natural radioactivity from air to different parts of plants. The maximum of deposit was measured on salient branches of trees, especially on the tips of conifer needles. The electric deposition of radioactive cluster ions can be switched off when the tree is insulated from the ground and connected to positive term of a HV voltage source. In such a experiment the radioactivity of tips of spruce needles was measured below 0.5 kBq/kg. The radioactivity of top needles of a 1.5 m high grounded spruce in natural atmospheric electric field was 3 kBq/kg. The electric field is stronger on tops of high trees where higher radioactivity is expected. Especially strong field is present under HV power transmission lines. On the tops of spruces under HV power line the radioactivity up to 20 kBq/kg was measured.

At least half of the radon daughters in air are carried by aerosol particles. The role of electric mechanism of deposition of airborne particles on the various elements of plant canopy can be estimated using the concept of critical electric field. If the actual electric field is comparable with or larger than the critical field, then the electric mechanism should not to be neglected. The value of the critical electric field depends on many factors and cannot be exactly calculated. This value can be only approximately estimated by using a simplified model in which the deposition target is replaced by a thin conducting wire.

The nanometer particles of diameter below of 10 nm are mostly neutral and the Brownian diffusion is the dominating mechanism of dry deposition at the normal atmospheric conditions. Aerodynamic deposition is the dominating mechanism for particles of diameter over 200 nm. The electric mechanism is important in the transition size range of 10–200 nm, which contains most of atmospheric aerosol particles.

The role of electric deposition is most important in case of low wind and on sharp structures like conifer needles, spider webs and insect antennas. Thus the environmental effect of the electric mechanism of aerosol deposition is the redistribution of the deposit on the elements of biological structures. Knowledge of deposition geometry improves our understanding of air pollution damage to plants. In particular, electric deposition of aerosol

particles should be considered when discussing enhanced pollution damage to the top branches of conifer trees. The electric field should not to be neglected when discussing the appearance and effect of radon daughters in the environment.

References

Butterweck, G. (1991) *Natürliche Radionuclide als Tracer zur Messung des turbulenten Austaushes und der trockenen Deposition in der Umwelt*. Doktordissertation, Universität Göttingen.

Ceburnis, D. and Steinnes, E. (2000) Conifer needles as biomonitors of atmospheric heavy metal deposition: comparison with mosses and precipitation, role of the canopy, *Atmos. Environ.*, **34**, 4265—4271.

Eckert, E.R.G., and R.M. Drake (1972) *Analysis of Heat and Mass Transfer*, McGraw-Hill, Tokyo.

Eisele, F.L. (1989) Natural and anthropogenic negative ions in the troposphere, *J. Geophys. Res*., **94D**, 2183–2196.

Eisele, F.L. (1989) Natural and transmission line produced positive ions, *J. Geophys. Res*., **94D**, 6309–6318.

Elster, J. and Geitel, H. (1902) Beschreibung des Verfahrens zur Gewinnung vorübergehend radioaktiver Stoffe aus der atmosphärischen Luft. *Phys. Z*., **3**, 305–310.

Fews, A.P., Henshaw, D.L., Keitch, P.A., Close, J.J., Wilding, R.J. (1999a) Increased exposure to pollutant aerosols under high voltage power lines. *Int. J. Radiat. Biol.* **75**, 1505−1521.

Fews, A.P., Henshaw, D.L., Wilding, R.J., Keitch, P.A. (1999b) Corona ions from powerlines and increased exposure to pollutant aerosols. *Int. J. Radiat. Biol.* **75**, 1523−1531.

Fuchs, N.A. (1964) *The Mechanics of Aerosols*, Pergamon Press, Oxford.

Henshaw, D.L., Ross, A.N., Fews, A.P., and Preece, A.W. (1996) Enhanced deposition of radon daughter nuclei in the vicinity of power frequency electromagnetic fields. *Int. J. Radiat. Biol.*, **69**, 25–38.

Hoppel, W.A., and Frick, G.M. (1990) The nonequilibrium character of the aerosol charge distributions produced by neutralizers. *Aerosol Science and Technology* **12**, 471–496.

Incropera, F.P., DeWitt, D.P. (1996) *Fundamentals of Heat and Mass Transfer*. John Wiley, New York.

Israël, H. (1973) *Atmospheric electricity*, vol. II. Israel Program for Scientific Translations, Jerusalem.

Jeffers, D. (1999) Atmospheric electric fields and radon daughter deposition on vegetation, *Radiat. Prot. Dosimetry*, **82**, 55–57.

Jonassen, N. (1988) Ions, electric fields and radon daughters effects of filtration and electrostatic plateout. In *Seventh Int. Congr. Int. Radiat. Prot. Assoc*., 377–380, Sidney.

Miles, J.C.H. and Algar, R.A. (1997) Measurement of radon decay product concentration under power lines. *Radiat. Prot. Dosim*., **74**, 193–194.

Moeller, D.W. (1986) *Method and apparatus for reduction of radon decay product exposure.* US Patent No. 4,596,585.

Porstendörfer, J, Zock, C., Reineking, A. (2000) Aerosol size distribution of the radon progeny in outdoor air. *Journal of Environmental Radioactivity* **51**, 37–48.

Porstendörfer, J. (1994) Properties and behavior of radon and thoron and their decay products in the air. *J. Aerosol Sci*., **25**, 219–263.

Holm, E., ed. (1994) *Radioecology. Lectures in Environmental Radioactivity*. World Scientific, Singapore, New Jersey, London, Hong Kong.

Reischl, G.P., J.M. Mäkelä, R. Karch, and J. Necid (1996) Bipolar charging of ultrfine particles in the size range below 10 nm, *J. Aerosol Sci*., **27**.

Schneider, T., Bohgard, M., and Gudmundsson, A. (1994) A semiempirical model for particle deposition onto facial skin and eyes. Role of air currents and electric fields. *J. Aerosol Sci*., **25**, 583–593.

Tammet, H. (1991) Aerosol electrical density: interpretation and principles of measurement, *Report Series in Aerosol Sci*., Helsinki, **19**, 128–133.

Tammet, H. and Israelsson, S. (1999) Atmospheric electricity as a factor of dry deposition of particulate pollution. *Proc. 11th Int. Conf. Atmos. Electr*., NASA, MSFC, 622–625.

Tammet, H. (1995) Size and mobility of nanometer particles, clusters and ions. *Journal of Aerosol Science* **26**, 459–475.

Tammet, H., and V. Kimmel (1998) Electrostatic deposition of radon daughter clusters on the trees, *J. Aerosol Sci*., **29**, S473–S474.

Tripathi, S.N., and R.G. Harrison (1998) Dry deposition of electrically charged aerosols, *J. Aerosol Sci*., **29**, S809-S809.

Wasiolek, P.T., James, A.C. (2000) Unattached fraction measuring technique and radon lung dose. *Journal of Environmental Radioactivity* **51**, 137–151.

Weseley, M.L., Hicks, B.B. (2000) A review of the current ststus of knowledge on dry deposition. *Atmospheric Environment* **34**, 2261–2282.

Wessel, R.A., and J. Righi (1988) Generalized correlations for inertial impaction of particles on a circular cylinder, *Aerosol Sci. Technol*., **9**, 29–60.

Wilkening, M.H. (1977) Influence of the electric fields of thunderstorms on radon-222 daughter ion concentrations. In *Electrical Processes in Atmospheres*, 54–59, Steinkopff, Darmstadt.

Willett, J. (1985) Atmospheric-electrical implications of ^{222}Rn daughter deposition on vegetated ground. *J. Geophys. Res. D*, **90**, 5901–5908.